American Mineralogist, Volume 61, pages 470–483, 1976

Stacking disorder and polytypism in zussmanite

DAVID A. JEFFERSON[1]

Department of Mineralogy and Petrology
Downing Place, Cambridge, England

Abstract

The stacking disorder observed in zussmanite has been investigated by X-ray diffraction methods. Two types of disorder have been found, one corresponding to a moderately disordered version of the accepted rhombohedral structure, and the other to a severely disordered arrangement with triclinic symmetry. Electron probe microanalysis has shown that these states correspond to compositions approaching the ideal formula, $KFe_{13}Si_{17}AlO_{42}(OH)_{24}$, and one in which almost all potassium is removed and up to 3.5 percent manganese is substituted for iron. Detailed analysis of the disorder reveals that in the former state there is a distinct possibility of forming one-layer alternative polytypes with triclinic symmetry, and that in the latter, two-layer triclinic polytypes can form, the disorder being nonrandom in both cases. Subsequently six one-layer and three two-layer polytypes have been observed, but only the latter have been isolated. A possible origin of the disorder as a result of the removal of strain due to potassium ions is discussed, and polytype formation is suggested as resulting from the combined presence of disorder and strain in the structure.

Introduction

The existence of mineral structures exhibiting certain forms of crystallographic disorder has been known for many years. Mathematical models have been proposed for such systems, especially the displacement and substitutional disorders often found in layer silicates. The first general treatment in this field was that of Hendricks and Teller (1942), specialized cases of this theory being applied to close-packed structures by Wilson (1942) and others, and the theory has been modified to consider more complicated arrangements by Jagodzinski (1949), Gevers (1952), and Kakinoki and Komura (1965). Actual applications to mineral systems have been relatively few, but include the relatively simple study of cronstedtite by Shaw *et al.* (1965), with the more complex case of the intermediate plagioclases being given by Megaw (1960), and more recently, the study of vaterite by Meyer (1969). Numerous studies of disordered clay minerals have also been reported, a good account of these being given by Brindley (1961) and MacEwan *et al.* (1961).

The study of displacement stacking disorder in zussmanite formed part of a more general investigation of this type of disorder in layer silicates, the principal aim being to determine the type of disorder directly from the observed X-ray diffraction data, in a similar manner to that employed in a normal crystal-structure investigation. One part of this study, concerning stacking disorder in wollastonite, has already been reported (Jefferson and Bown, 1973). With zussmanite, the investigation had a much wider scope, a study of the disorder leading to the discovery of hitherto unreported polytypes of the basic zussmanite structure. A link between the presence of disorder in the structure and ionic substitution was also investigated.

Structure

Zussmanite was discovered in 1960 by S. O. Agrell, and in a preliminary investigation by Agrell *et al.* (1965) was given the ideal formula $KFe_{13}Si_{17}AlO_{42}(OH)_{14}$, and assigned to space group $R3$ or $R\bar{3}$ with a triple hexagonal cell of dimensions $a = 11.66$ Å and $c = 28.69$ Å. Zussmanite was shown to be a new type of layer silicate by Lopes-Vieira and Zussman (1969). A plan of one layer of their structure (hereafter referred to as the LZ structure) is shown in

[1] Present address: Edward Davies Chemical Laboratories, The University College of Wales, Aberystwyth, SY23 1NE, U.K.

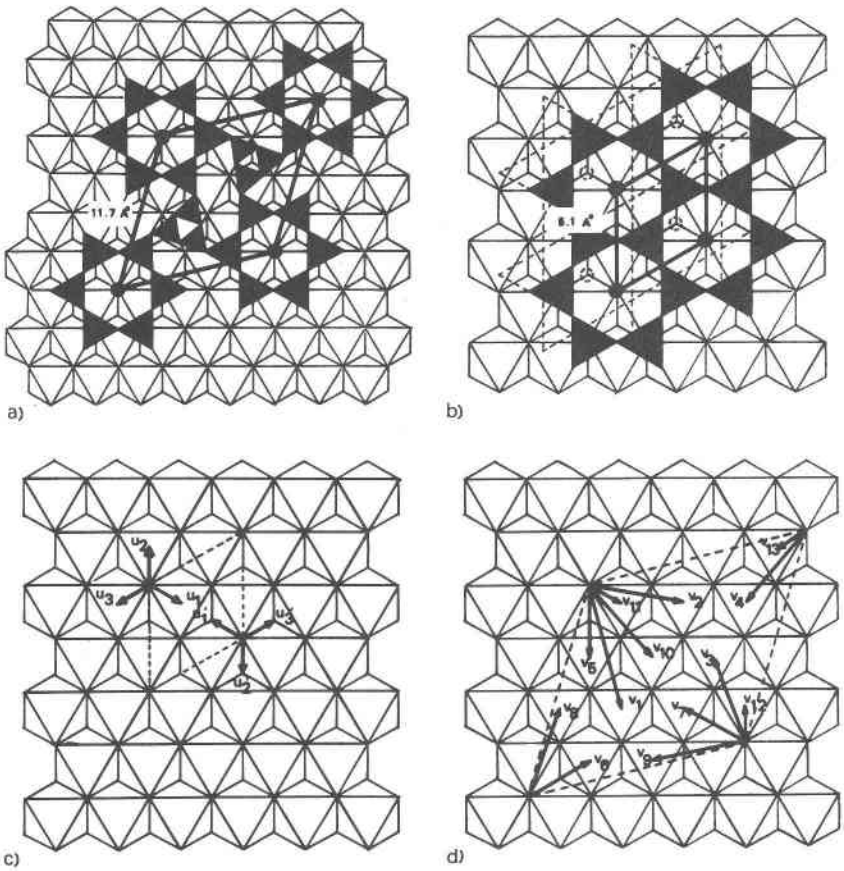

FIG. 1. (a) Idealized projection onto the plane of the layers of one zussmanite layer in terms of coordination polyhedra, (b) similar projection for the ideal mica layer, (c) displacement vectors in mica, outlined against the octahedral component, (d) displacement vectors in zussmanite.

idealized form in Figure 1a, together with an idealized projection of a mica layer for comparison (Fig. 1b).

In micas the structural layers consist of an octahedral component, essentially two close-packed planes of O^{2-} and OH^- anions, with cations situated in the octahedral interstices. Filling of only two-thirds of or all of the interstices produces di- and tri-octahedral micas respectively. The octahedral component is flanked on each side by tetrahedral components, consisting of infinite sheets of six-membered rings of inwardly-pointing SiO_4 tetrahedra, with the apical O^{2-} anions of those tetrahedra being part of the close-packed layers in the octahedral component. Complete structural layers are bonded to one another by large cations situated betwen six-membered rings on the adjacent sides of neighboring layers.

Similarly, in zussmanite the layers consist of an octahedral component, in this case trioctahedral, flanked by tetrahedral components, but differ from those in micas in that the tetrahedral components are not continuous sheets of six-membered rings. Instead, those rings are isolated from one another, and are linked by three-membered rings of tetrahedra, which are above the plane of six-membered rings and are also bonded to the six-membered rings of the next layer. Hence there are silicon–oxygen bonds between layers, in addition to potassium cations situated, as in micas, between six-membered rings on the upper and lower surfaces of adjacent layers. The non-continuous nature of the tetrahedral component necessitates a larger repeat unit in the plane of the layers than in micas, and the unit cell is correspondingly larger. Eggleton (1972) has recently shown that the structure of stilpnomelane is constructed along similar, although more complex lines.

Two of the most interesting features of layer silicates are the large numbers of polytypic[2] structures observed and the frequent occurrence of stacking disorders, which in micas have been interpreted as extremely fine intergrowths of different polytypes (Smith and Yoder, 1956). Both features arise from the method of construction of the layers. In the idealized mica structure no displacement of one complete layer relative to another can occur at the level of the interlayer cations, since the six-membered rings on adjacent layers must superimpose directly to accommodate those cations. However, within any given layer, some offset between tetrahedral networks on the upper and lower surfaces is inevitable, owing to the fact that the octahedral component consists of two sheets of close-packed ions. In the mica structure three different offsets or displacement vectors (Fig. 1c) are immediately obvious and are designated $\mathbf{U}_{1-3}$. Three additional vectors $\mathbf{U}'_{1-3}$ are possible if the octahedral component is rotated through 180°. When the layers are stacked in the crystal, the displacement vectors employed in subsequent layers determine the polytype obtained, and where the sequence of vectors is not regular, a stacking disorder results.

With zussmanite, owing to the more complex repeat unit within the layers, the number of different displacement vectors possible is much greater (Fig. 1d), there being thirteen, designated $\mathbf{V}_{1-13}$ and a further thirteen, $\mathbf{V}'_{1-13}$ if allowance is made for 180° rotation of the octahedral component in successive layers. In the LZ structure all the layers are stacked by the vector $\mathbf{V}_1$, components (2/3, 1/3) producing a rhombohedral lattice which in the course of this investigation was given the designation $3R$ (1). Lopes-Vieira and Zussman observed that considerable stacking disorder was present in the structure, as shown by streaks in the reciprocal lattice perpendicular to the plane of the layers, and attributed this to the occasional use of alternative displacement vectors. The principal object of this study was to investigate the arrangement and possible causes of these 'stacking mistakes'.

Disorder

Rotation of octahedra

A diagram of the reciprocal lattice of zussmanite, projected onto the plane of the layers, is shown in Figure 2. Lopes-Vieira and Zussman found that all reflections showed some degree of streaking parallel to c^*, except those with indices obeying the condition $k = 3h \pm 13n$, which were sharp and relatively stronger than the rest. Such sharp, strong reflections are another common feature of layer silicates, and have been explained as arising from planes within the structure which can be indexed on a 'sub-cell' having the same height as the conventional cell, but with a and b axes parallel to and equal in magnitude to the octahedron edges. In the LZ structure this sub-cell also has rhombohedral symmetry, and as the arrangement of successive octahedral components is rhombohedral irrespective of which of the displacement vectors $\mathbf{V}_{1-13}$ is used, spots corresponding to this sub-cell will always be sharp. Sub-cell spots of this type can only be streaked out parallel to c^* if rotation of successive octahedral components occurs, upsetting the rhombohedral stacking arrangement of octahedra.

For the initial examination, four samples of zussmanite, all from the same locality but from different mineral assemblages, were supplied by Dr. S. O. Agrell, Department of Mineralogy and Petrology, University of Cambridge[3]. X-ray oscillation examination showed a wide variation in the strength of the

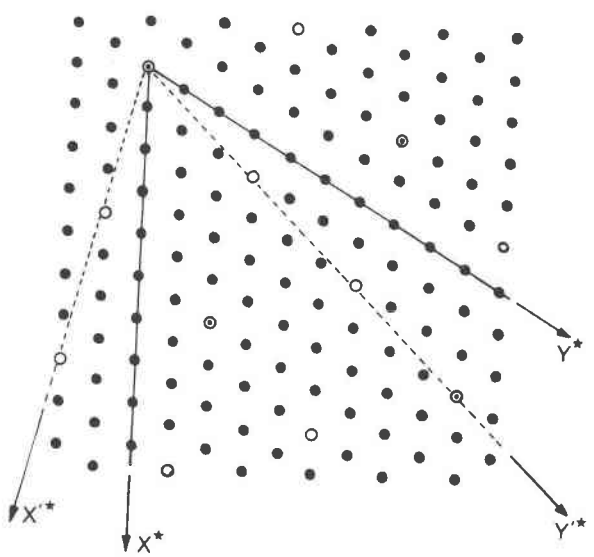

FIG. 2. Reciprocal lattice of zussmanite projected onto the plane of the layers, showing the true cell and the sub-cell.
●—general reflections
○—general sub-cell reflections
⊙—sub-cell reflections obeying the condition $2h + k = 3n$

[2] The term 'polytypism' throughout this paper refers to structures which are based upon different stacking arrangements of structurally similar but not necessarily identical layers.

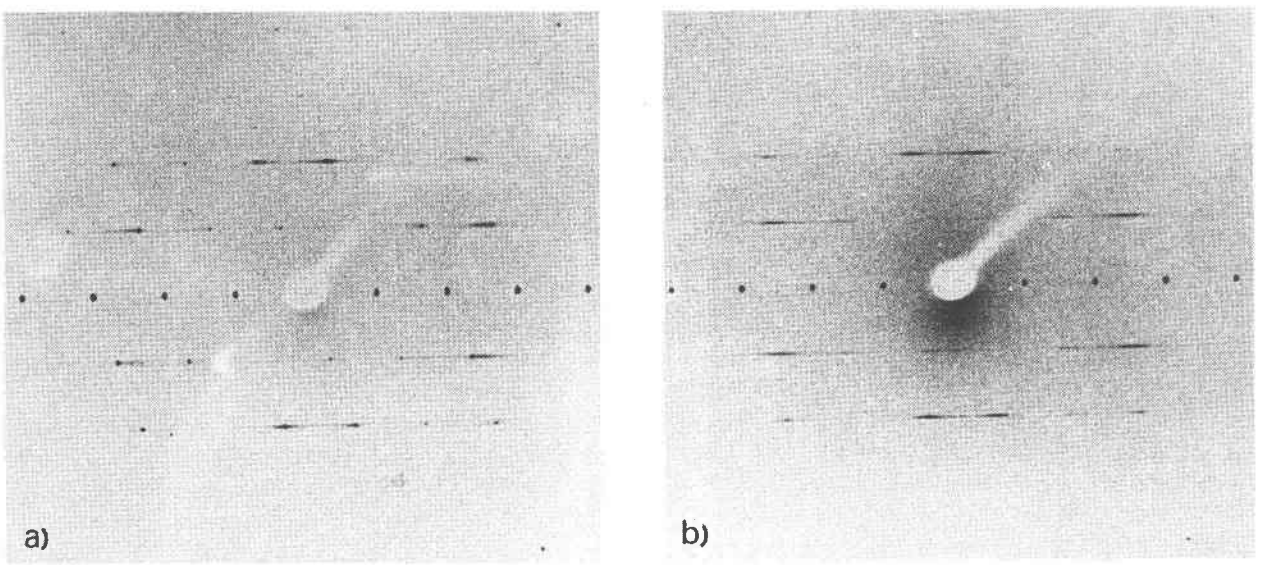

FIG. 3. Zero-level, *a*-axis precession photographs of zussmanite. a) moderately disordered rhombohedral type. b) severely disordered triclinic type (monochromatic cobalt $K\alpha$ radiation, 30 kV, 20 mA)

diffuse streaks exhibited by the crystals studied, and hence of the degree of disorder present. None of the crystals selected could be described as completely perfect, although two closely approached this ideal, but most showed considerable disorder and some gave very little indication of any rhombohedral maxima on the diffuse streaks. Several of the more severely disordered crystals were examined in greater detail by Weissenberg methods to try and find evidence for 180° rotation of successive octahedral components, and in a few cases a very slight streaking of sub-cell maxima was observed. In these cases faint extra maxima appeared along the sub-cell rows corresponding to the alternative rhombohedral orientation, but there was no evidence to indicate any possibility of structures having ordered rotations of the octahedral components. It is true for most micas also, that mixtures of 0° and 180° rotations do not occur in the octahedral components, and Radoslovich (1963) attributed this to the nonhexagonal nature of the six-membered rings within the structure. Where the six-membered rings in micas show near-hexagonal symmetry, as in fluor-polylithionite (Takeda and Burnham, 1969), polytypes based on successive rotations do occur, and recent studies by Zhouklistov *et al.* (1973) have shown that this can occur in micas with nonhexagonal rings. The Radoslovich explanation cannot hold for zussmanite, however, since the six-membered rings are very nearly hexagonal. In all the crystals examined, the sub-cell spots obeying the condition that $2k + h = 3n$ were perfectly sharp, even when other sub-cell reflections showed slight streaking. These $2h + k = 3n$ reflections corresponded to planes in the structure unaffected even by rotations of the octahedral components, and would only be streaked if there were variations in the interlayer spacing.

Range of disorder observed

When crystals were examined on a precession instrument to show the streaks in greater detail, it was evident that two extremes of disorder existed in the material. These are illustrated by the zero-level *a*-axis precession photographs of Figure 3. The first type, which was the most common, could be described as a disordered rhombohedral arrangement, still retaining the rhombohedral spots but not always having true rhombohedral symmetry if the actual shapes of the streak profiles were considered. The second type was triclinic, with no trace of rhombohedral spots, and only very broad maxima on the streaks, it being impossible to find any simple lattice corresponding to these maxima. Some crystals appeared to represent an intermediate stage between these two extremes.

[3] Specimen numbers A2125 and A2138 (Collectors Nos.) and 102459 and 102480 (Mineralogical Museum, University of Cambridge).

The exact symmetry in each case was determined by recording the zero- and first-level precession photographs with the [100], [110] and [010] directions in the triple hexagonal cell as the precession axis.

When observed optically in thin sections, many crystals of zussmanite showed a marked change in birefringence along lines parallel to the basal cleavage, and this has been attributed to a pronounced zoning of manganese by Agrell and Long (unpublished). All the crystals initially used for X-ray examination were from crushed samples, so some single crystals were then removed from thin sections. Before being mounted on the precession instrument, these crystals were carefully cleaved to separate the parts of different birefringence, which were then examined separately. Without exception the outer margins of the crystals showed the near-complete disorder of Figure 3b, while the central regions gave the rhombohedral-type pattern of Figure 3a. The effect was subsequently noted on crystals from crushed samples which were cleaved in the same manner, and careful cleaving of a relatively large crystal into several pieces, each fragment being examined in turn, showed that the change in the type of disorder occurred suddenly at the boundary between the regions of different birefringence, there being no gradual transition.

Microprobe analysis

Several crystals from thin sections were examined in the manner described above, and were subsequently transferred to and mounted upon glass slides, polished, and analyzed by the electron microprobe using the method of Sweatman and Long (1969). Analyses of these fragments, and of some of the crystals from crushed samples which were also examined, varied considerably from the original chemical analysis of Agrell *et al.* (1965). The variation in manganese content originally noted by Agrell and Long was found to be from 0.5 to 3.5 weight percent, and a related variation in the potassium and aluminum contents was also observed. These relations can be seen by plotting the weight percentages of manganese against those of potassium and aluminum, as in Figure 4. The analyses fall into two main groups, corresponding to fragments of the crystals

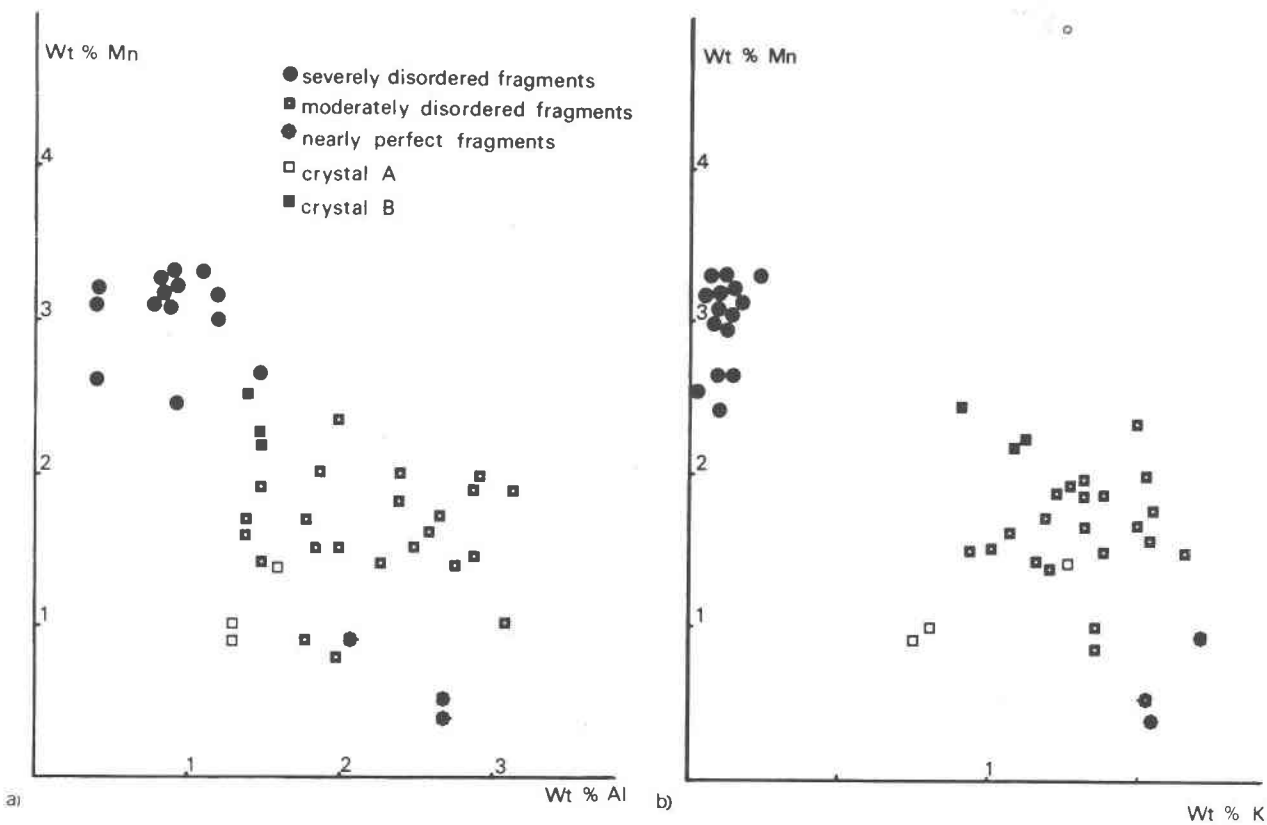

FIG. 4. Weight percentages of manganese plotted against those of (a) aluminum and (b) potassium. Crystals *A* and *B* refer to the rhombohedral and triclinic crystals used in the detailed X-ray study of the disorder.

from the outer edges parallel to the basal cleavage, and those fragments from the central regions. Edge fragments, with a manganese content of approximately 2.5 to 3.5 weight percent, and aluminum and potassium contents of 0.0 to 1.0 and 0.0 to 0.25 weight percentages respectively, were those giving the severely disordered triclinic patterns, whereas the central fragments showing the moderately disordered rhombohedral patterns possessed manganese, aluminum and potassium contents of 0.0 to 2.0, 1.0 to 3.0 and 1.0 to 1.5 weight percentages respectively. The analyses of crystals from crushed samples also showed the same behavior, those giving well-ordered X-ray diffraction patterns having low manganese and high potassium and aluminum contents, whereas the severely disordered crystals showed the opposite characteristics. A clear link could therefore be seen between the degree and type of disorder present and the variation of manganese and potassium/aluminum content in these crystals.

The variation in the disorder across crystals in thin section was also observed by electron diffraction. Sections containing zussmanite crystals were thinned by ion bombardment (Barber, 1970) and examined in an AEI EM6G electron microscope, enabling the variation in the degree of disorder to be observed in the selected-area diffraction mode. Although the diffraction patterns obtained always appeared to be relatively heavily disordered, a distinction could still be drawn between the two types of pattern, and it was again noted that the change in the type of disorder present occurred relatively suddenly on scanning across the crystals. More recently, this change in the degree of disorder has been observed directly by bright-field lattice resolution techniques (Jefferson and Thomas, 1974).

X-ray analysis

Experimental

To try to understand more completely the nature of the stacking processes occurring within each type of disordered crystal, an attempt was made to investigate the disorder directly using the method of Zachariasen (1947). This method leads to the determination of an 'average Patterson function' of the type first described by Cochran and Howells (1954), showing the average disposition of neighboring layers in the structure with respect to any given layer. It was hoped that, as in the complementary study of wollastonite, this approach would give information about first- and second-neighboring layers in each crystal much more readily than the trial and error construction of various models to explain the observed streak profiles. Crystals representative of each extreme of disorder were chosen, and three-dimensional data for both crystals were collected by the precession method, using monochromatic cobalt $K\alpha$-radiation. Streak profiles were measured on a densitometer, and corrected for Lorentz and polarization factors, using a modified version of the polarization correction given by Azaroff (1955). No allowance for deviation of the polarization factor of the plane graphite monochromator from its ideal value such as that described by Hope (1971) was made, as it was felt that the accuracy of the measurements was insufficient to warrant such a correction. Measurements were corrected for absorption and experimental broadening using the methods of Wuensch and Prewitt (1965) and Stokes (1948), the corrected profiles being divided by the form-factor $|G|^2$, of one layer of the LZ structure to obtain 'unitary' intensity profiles, $|G|^2$ being evaluated as a continuous function in reciprocal space. For both crystals rows of spots with $k = 3h + 13n$ were completely sharp.

If it is assumed that the displacement vectors have the ideal values of Figure 1d, it can be shown that there are six unique unitary intensity profile shapes for a triclinic crystal, and only two for a rhombohedral crystal, all unitary profiles having one of these shapes, although displaced by varying amounts in the c^* direction. The measured unitary profiles were therefore classified into these six (or two) types, averaged to give mean unitary intensity profiles, and then Fourier inverted to give average Patterson functions. As the intensity distribution in reciprocal space was continuous only along rows parallel to c^*, the inverse transformation was effectively

$$P(u, v, w) = \sum_{hk}\sum \int_{-1/2}^{1/2} I_{hk}(l) \exp(-2\pi i l w)\, dl \cdot \exp[-2\pi i(hu + kv)]$$

$I_{hk}(l)$ being the unitary intensity profile for a given h and k. The integral part was first evaluated for each of the six mean unitary profiles, using $w = 1, 2, 3, 4$, producing Patterson coefficients, which when included in the associated summation, synthesized the first four sections of the average Patterson function. In practice, assuming the ideal displacement vectors, only the weights of the thirteen peaks in each section had to be evaluated, and using the real and imaginary parts of the six Patterson coefficients, plus the fact that rows of spots with $k = 3h + 13n$ were completely

sharp, a system of equations could be set up to solve for the required peak weights. Estimates of limits of error in these weights could then be made by carrying out the integral part of the transformation for each of the unitary profiles before averaging, giving limits of error in the Patterson coefficients which could then be used to calculate limits of error in peak weights.

The average Patterson functions give, for all possible displacement vectors, the probability that the next layer after any given layer will be stacked with that particular displacement, and the same for the next but one, and successive layers. They have been interpreted as far as possible in terms of the existence and continuing probabilities of Kakinoki and Komura (1965), full details of the process of interpretation being reported elsewhere (Jefferson, 1973). An existence probability like f_{ijk} is the probability that any sequence of three successive displacement vectors in the crystal will be $\mathbf{V}_i\mathbf{V}_j\mathbf{V}_k$. A continuing probability, such as p_{ijkl}, is the probability that a sequence $\mathbf{V}_i\mathbf{V}_j\mathbf{V}_k$ will be immediately followed by $\mathbf{V}_l$. Obviously, $p_{ijkl} = f_{ijkl}/f_{ijk}$. f_l gives the proportion of displacement vectors $\mathbf{V}_l$. In a crystal for which the displacement vectors are randomly distributed, the continuing probability for any sequence of vectors ending in $\mathbf{V}_i$ is f_i, the extent to which p_{ii}, p_{ji}, *etc.* differ from f_i being a measure of the short-range order of displacement vectors. Models resulting from the final interpretation process were used to calculate theoretical mean profiles, these being shown alongside the experimentally measured ones in Figure 5.

Rhombohedral type

It could be definitely established that the vectors $\mathbf{V}_{1-4}$ occurred in both crystals, and that $\mathbf{V}_{8-10}$ occurred in the moderately disordered rhombohedral example, but within the maximum limits of error of the Patterson peaks the existence of the last three vectors could not be conclusively established in the triclinic form. The best overall solutions for both crystals are shown in Table 1, values of all existence and continuing probabilities involving the vectors

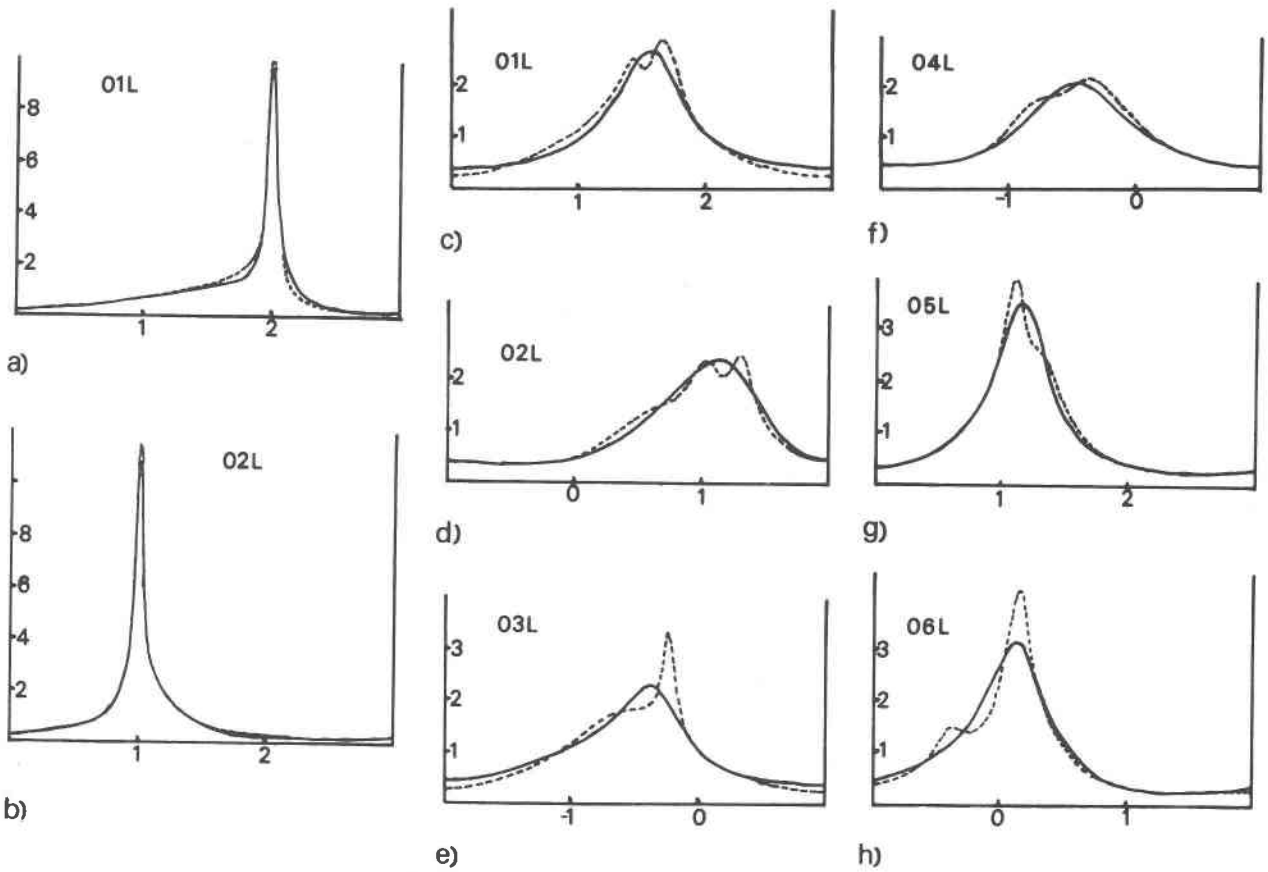

FIG. 5. Measured (dashed lines) and computed (solid lines) mean streak unitary intensity profiles for the crystals used in the detailed X-ray study; *a* and *b*—rhombohedral crystal, *c* to *h*—triclinic crystal.

TABLE 1. Final existence and continuing probabilities for both zussmanite crystals studied

Rhombohedral Crystal		
Sequence	f	p
1	0.628(21)*	0.628(21)
2	0.109(11)	0.109(11)
3	0.109(11)	0.109(11)
4	0.109(11)	0.109(11)
11	0.487	0.775
12	0.041	0.065
13	0.041	0.065
14	0.041	0.065
21	0.041	0.372
22	0.034	0.312
23	0.013	0.119
24	0.013	0.119
31	0.041	0.372
32	0.013	0.119
33	0.034	0.312
34	0.013	0.119
41	0.041	0.372
42	0.013	0.119
43	0.013	0.119
44	0.034	0.312
111**	0.408	0.838
112	0.021	0.044
113	0.021	0.044
114	0.021	0.044
211	0.021	0.525
212	0.009	0.217
213	0.005	0.113
214	0.005	0.113
311	0.021	0.525
312	0.005	0.113
313	0.009	0.217
314	0.005	0.113
411	0.021	0.525
412	0.005	0.113
413	0.005	0.113
414	0.009	0.217
1111	0.365	0.894
1112	0.010	0.025
1113	0.010	0.025
1114	0.010	0.025
2111	0.010	0.481
2112	0.004	0.164
2113	0.004	0.164
2114	0.004	0.164
3111	0.010	0.481
3112	0.004	0.164
3113	0.004	0.164
3114	0.004	0.164
4111	0.010	0.481
4112	0.004	0.164
4113	0.004	0.164
4114	0.004	0.164

Triclinic Crystal		
Sequence	f	p
1	0.398(26)	0.398(26)
2	0.230(25)	0.230(25)
3	0.195(28)	0.195(28)
4	0.145(25)	0.145(25)
11	0.150	0.377
12	0.087	0.219
13	0.083	0.208
14	0.059	0.148
21	0.087	0.378
22	0.078	0.339
23	0.029	0.127
24	0.032	0.138
31	0.083	0.424
32	0.029	0.149
33	0.060	0.308
34	0.021	0.106
41	0.059	0.403
42	0.032	0.217
43	0.021	0.142
44	0.029	0.199

*Maximum limits of error (x 10^3)
**Probabilities for sequence involving three or more layers are given only when different from those expected from a two-layer model. All probabilities involving the vectors V_{8-10} are neglected.

$\mathbf{V}_{8-10}$ being omitted, as these accounted to at most less than five percent of the total displacement vectors in the crystals. Limits of error in f_i values were determined directly from the limits of error of the corresponding Patterson peaks, but errors could not be so readily evaluated for f_{ij}, f_{ijk}, and f_{ijkl} values, which were calculated from higher terms in the average Patterson. However, little change in the overall values of existence and continuing probabilities was noted when the peaks in these higher terms were adjusted to the extremes of their limits of error, which ranged from five percent in the large peaks to almost forty percent in the smaller ones.

For the disordered rhombohedral crystal, the probability of a sequence of consecutive $\mathbf{V}_1$ vectors being further extended increased with the length of the sequence up to a four-layer sequence at least, as shown by the gradually increasing values of p_{11}, p_{111}, and p_{1111}. Similar behavior was found for the vectors $\mathbf{V}_2$, $\mathbf{V}_3$, and $\mathbf{V}_4$, p_{22}, and hence p_{33} and p_{44} being considerably greater than f_2, f_3, and f_4 respectively, but no significant increase of p_{222} with respect to p_{22} could be detected, indicating that the clustering of layers stacked by $\mathbf{V}_2$-type vectors was not as pronounced as that found with layers stacked by $\mathbf{V}_1$. Little increase in the values of p_{23}, p_{34}, and p_{24} was shown over those expected for a random structure, indicating no great tendency to form structures containing ordered se-

quences of different $\mathbf{V}_2$-type vectors, and sequences involving $\mathbf{V}_{8-10}$ were of such low probability that few conclusions could be drawn regarding their role in the crystal. When vector combinations of the $\mathbf{V}_1\mathbf{V}_2$-type were considered, p_{12}, p_{13}, and p_{14} indicated a general tendency against the formation of structures containing such sequences, but examination of continuing probabilities of the type p_{112}, p_{1112}, and p_{212} suggested that although a vector of the $\mathbf{V}_2$-type was not, in general, favored after a $\mathbf{V}_1$-vector, $\mathbf{V}_2$-type vectors did have a higher continuing probability than that expected from a random model when following a vector sequence like $\mathbf{V}_2\mathbf{V}_1$. This implies a tendency to continue such $\mathbf{V}_1\mathbf{V}_2$ sequences once they have been initiated, however unfavorable it might be to start such a sequence.

The disordered rhombohedral crystal can therefore be regarded as fine intergrowths of the rhombohedral $3R(1)$ form of zussmanite and three different, but symmetry-related, triclinic polytypes, designated $1Tc(2)$, $1Tc(3)$, and $1Tc(4)$[4], employing repeated use of the displacement vectors $\mathbf{V}_2$, $\mathbf{V}_3$, and $\mathbf{V}_4$ respectively. At the interfaces between these and the $3R(1)$ polytype, there is a definite, although small, possibility of tiny regions of triclinic polytypes involving two-layer repeats of the type $\mathbf{V}_1\mathbf{V}_2$ being formed, structures of this type being designated $2Tc(1, 2)$, $2Tc(1, 3)$, and $2Tc(1, 4)$.

Triclinic type

When the severely disordered triclinic crystal was examined, agreement between experimental and calculated mean unitary profiles was worse than that for the rhombohedral crystal. This was largely because the analysis could not be taken so far, there being no strong trends towards ordering of displacement vectors, such as those shown by $\mathbf{V}_1$ vectors in the rhombohedral example, to aid in the interpretation of higher terms in the Patterson function. The peaks shown in the experimental profiles of the triclinic crystal were also of no assistance, as they could not be assigned to either a single lattice, or a superposition of several lattices, and hence corresponded to no definite polytypic modification. The disposition of displacement vectors was, however, clearly different from that of the first crystal, with more than half of the layers being stacked by vectors other than $\mathbf{V}_1$. The probability of sequences of consecutive $\mathbf{V}_1$ vectors was actually less than that expected from a completely random model, p_{11} being less than f_1, and a slight but definite tendency towards the formation of sequences of the type $\mathbf{V}_1\mathbf{V}_2$ was noted, irrespective of the vectors preceding $\mathbf{V}_1$. Sequences of the $\mathbf{V}_2\mathbf{V}_2$ type were however still favored, but not by so great a margin as in the first crystal. As with the rhombohedral example, the continuing probabilities of $\mathbf{V}_2\mathbf{V}_3$-type sequences were more of less those expected from a completely random model, and no definite conclusions could be drawn concerning sequences involving the vectors $\mathbf{V}_{8-10}$.

This second crystal is thought to be a further stage in the overall variation of disorder in zussmanite, where regions of $3R(1)$ and $1Tc(2)$-type structures are so small that interfaces between them are just as important, giving rise to a greater preponderance of $2Tc(1, 2)$-type structures. Although the degree of disorder present (measured by the proportion of layers with displacements other than $\mathbf{V}_1$) has increased in this crystal, this increase is not just towards a greater randomness, but also involves a definite change in the type of short-range order observed.

Isolation of polytypes

In the initial examination, some crystals had been observed to show faintly discernible extra maxima along the streaks, although these were too faint to index. In view of the evidence obtained for polytype formation in the detailed X-ray study, a systematic examination of over fifty crystals was made, to try to find macroscopic examples of these alternative structures. The results of this examination are given in Table 2. Although most crystals showed only the $3R(1)$ structure, some gave zero-level precession photographs of the type shown in Figure 6a, with the principal extra spots being due to the polytypes $1Tc(2)$, $1Tc(3)$, and $1Tc(4)$. In some cases spots due to the polytypes $1Tc(8)$ and $1Tc(10)$ were noted, but some spots remained unexplained. Apart from the extra spots, the streak profile shapes in this type of crystal resembled those of Figure 3a. In all cases the positions of the extra spots, relative to the $(00l)$ maxima which were common to all polytypes, were measured with a travelling microscope and compared with spot positions calculated for each of the alternative one-layer polytypes (Figure 6b). No spots due to the polytypes $1Tc(5\text{–}7)$ and $1Tc(11\text{–}13)$ were ever observed, nor were any of the one-layer polytypes ever

[4] In the previously published study of wollastonite the one-, three- and four-layer triclinic polytypes were designated $1T$, $3T$, and $4T$ respectively. Use of this notation could cause difficulties in zussmanite, where a trigonal structure, with ordered sequences of the type $\mathbf{V}_2\mathbf{V}_3\mathbf{V}_4$ is possible. Thereafter triclinic polytypes of zussmanite will therefore be referred to as $1Tc(2)$, $2Tc(1, 2)$, *etc.*, reserving the notation such as $3T$ for the truly trigonal structure.

found to occur singly, or in crystals not showing $3R(1)$ spots.

Some spots remained unexplained until a crystal giving a zero-level precession photograph of the type shown in Figure 6c was found. The spots in this photograph could not be explained by any of the one-layer triclinic forms, but fitted very well with the positions predicted for a two-layer polytype for which the displacement vector of the second layer was $\mathbf{V}'_{12}$. Six two-vector combinations would produce this unit cell, and hence the same spot pattern, namely $\mathbf{V}_1 + \mathbf{V}_3$, $\mathbf{V}_2 + \mathbf{V}_9$, $\mathbf{V}_4 + \mathbf{V}_6$, $\mathbf{V}_5 + \mathbf{V}_{12}$, $\mathbf{V}_7 + \mathbf{V}_{10}$, and $\mathbf{V}_{11} + \mathbf{V}_{13}$. To decide between these possibilities, the intensity distribution for each was calculated. On comparing these possibilities with the measured relative intensities, shown in Table 3, there was little doubt that the sequence $\mathbf{V}_1 + \mathbf{V}_3$ was correct, as indeed might have been expected following the analysis of the disordered crystals.

For this crystal a two-layer polytype occurred without $3R(1)$ spots being shown also, but other crystals showed spots from two-layer polytypes together with $3R(1)$ and one-layer triclinic maxima. All extra spots could be explained in this way, by including the polytypes $2Tc(1, 2)$, $2Tc(1, 3)$, and $2Tc(1, 4)$, calculated spot positions for these being shown in Figure 6d. No trace was found of any two-layer polytypes other than these, or of more complex structures.

TABLE 2. Distribution of polytypic structures in the crystals examined

Crystal	Disorder*	Symmetry**	Maxima observed
A2138.1	B	Tc	3R(1), 1Tc(8)
A2138.13	C	Tc	3R(1), 1Tc(2), 1Tc(8)
A2138.14/1	C	Tc	2Tc(1,2)
A2138.14/2	C	R	3R(1)
A2138.14/3	C	Tc	3R(1), 1Tc(8)
A2138.14/4	D	Tc	3R(1)
A2138.14/5	C	Tc	3R(1), 1Tc(2), 1Tc(8), 2Tc(1,2)
A2138.14/6	C	R	3R(1)
A2138.14/7	B	R	3R(1)
A2138.14/8	B	Tc	3R(1), 1Tc(8), 2Tc(1,2)
A2138.14/9	D	Tc	3R(1), 1Tc(2), 1Tc(8)
A2138.14/10	C	R	3R(1)
A2138.14/11	D	Tc	3R(1)
A2138.14/12	C	Tc	3R(1), 1Tc(2), 1Tc(8), 2Tc(1,2)
A2138.14/13	C	Tc	3R(1), 1Tc(2), 1Tc(8), 2Tc(1,2)
A2138.14/14	C	Tc	3R(1), 1Tc(2), 1Tc(8), 2Tc(1,2)
A2138.16	C	Tc	3R(1), 1Tc(2), 2Tc(1,2)
A2138.17	B	R	3R(1)
A2138.19	B	R	3R(1)
A2138.22/1	D	Tc	-- ***
A2138.22/2	B	Tc	3R(1), 1Tc(8), 2Tc(1,2)
A2138.25/1	B	R	3R(1)
A2138.25/5	B	Tc	3R(1), 1Tc(8)
A2138.26/1	C	R	3R(1)
A2138.26/2	D	R	-- ***
A2138.26/3	D	Tc	3R(1), 1Tc(2)
A2138.27	C	R	3R(1)
A2138.28/1	B	R	3R(1)
A2138.28/2	C	R	3R(1)
A2138.29/1	D	R	-- ***
A2138.29/2	B	Tc	3R(1), 1Tc(8)
A2138.30/1	D	R	3R(1)
A2138.30/2	B	R	3R(1)
A2138.30/3	B	R	3R(1)
A2138.30/4	D	R	-- ***
A2138.31/1	D	R	-- ***
A2138.31/2	B	R	3R(1)
A2138.32/1	D	R	-- ***
A2138.32/2	B	R	3R(1)
102459.7	B	Tc	3R(1), 1Tc(2)
102480.7	A	R	3R(1)
A2125.T	A	R	3R(1)

*Types of disorder: slight (A), moderate (B), heavy (C), and severe (D).
**Overall symmetry: rhombohedral (R), triclinic (Tc).
***Only diffuse maxima present.

Discussion

Influence of potassium ions

A clear correlation between the nature of the disorder present in zussmanite and the chemical composition was established, and this can be explained when the details of the LZ structure are examined. Because of the three-layer periodicity and $\mathbf{V}_1$ stacking vector throughout, the sequence of structural units along the c-axis of the hexagonal cell is: potassium ion/three-membered ring/three-membered ring/potassium ion. . . . . In the LZ structure the octahedral component is distorted out of the plane of the layers, this distortion being away from a potassium cation on one side and towards a three-membered ring on the other side of the layer. As there are potassium cations and three-membered rings on either side of the octahedral component, this component is therefore distorted alternately up and down. Owing to silicon–oxygen bonds between layers, the six-membered rings enclosing a potassium ion are comparatively close together, comparable O–O distances in ferriannite and zussmanite being 3.40 Å and 3.18 Å. The strain on the network accomodating these cations can therefore be expected to be high, and as suggested by Lopes-Vieira and Zussman, it seems probable that the structure alleviates this strain by placing successive potassiums as far apart as possible. This is achieved by repeated use of the $\mathbf{V}_1$ vector, adjacent potassiums being closer if any other vector is used. When the crystals become depleted in potassium, therefore, the tendency towards disorder will increase, as observed experimentally in the potassium-poor margins, due to the reduction in the strain involved in using other displacement vectors. Use of the vectors $\mathbf{V}_{5-7}$ and $\mathbf{V}_{11-13}$ would entail having adjacent potassium ions extremely close together, a most unfavorable situation, and hence these vectors would be almost totally absent, as found experimentally. Indeed, the strain involved in using these latter vec-

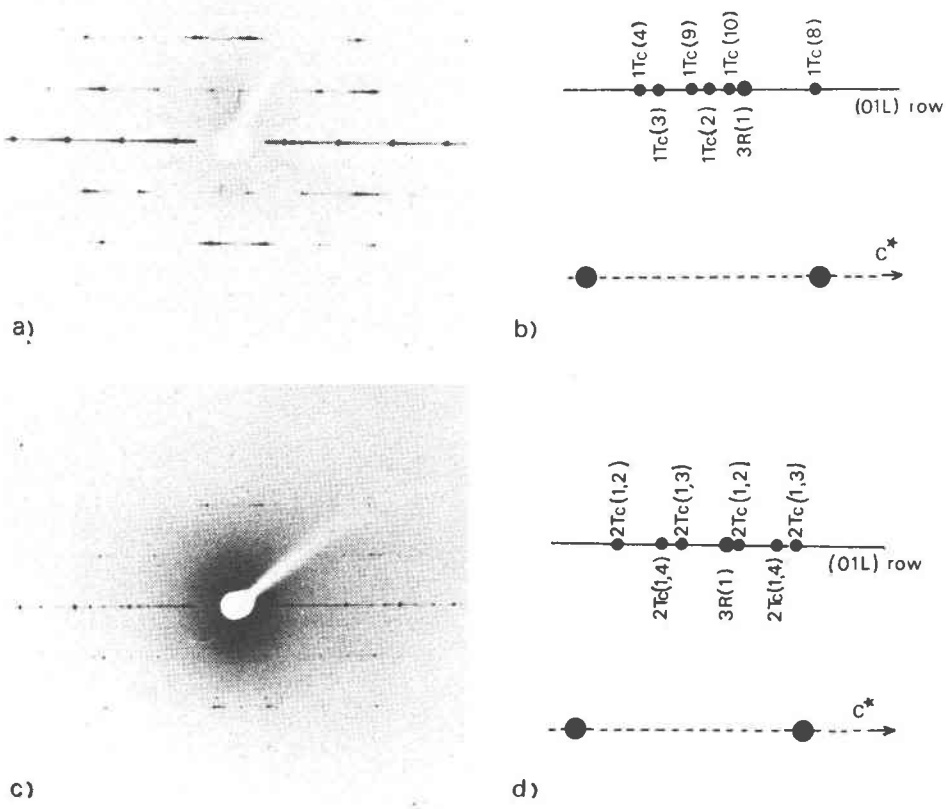

FIG. 6. (a) *a*-axis zero level precession photograph of a crystal showing mainly one-layer triclinic polytypes; (b) calculated spot positions for polytypes of the 1*Tc*(2)- and 1*Tc*(8)-type; (c) *a*-axis zero-level precession photograph of a crystal showing a two-layer triclinic polytype; (d) calculated spot position for polytypes of the 2*Tc* (1, 2)-type. (*a* and *c* taken with iron-filtered cobalt radiation, 30 kV, 20mA)

tors might be high even when all potassium is removed, as there was no evidence for their use in the severely disordered triclinic crystal studied.

Published values of ionic radii (Shannon and Prewitt, 1969) give the radii of Fe^{2+} and Mn^{2+} as 0.77 and 0.82 Å respectively. Increasing substitution of manganese into the octahedral component of the layers might therefore be expected to give a corresponding increase in cell dimensions, but this was not observed. Owing to the fact that the layers are constrained in the *ab* plane by the silicon–oxygen network, and that the high pressures under which zussmanite is believed to form would inhibit any increase in layer spacing, inclusion of manganese into the layers would therefore put more strain into an already quite severely strained network. However if, as in the outer margins of the crystal, there is a deficiency of potassium ions, then the removal of their associated strains would facilitate the incorporation of manganese into the layers, thus producing the observed composition relations.

The features described so far can be explained in terms of the strain due to adjacent potassium ions. When second-nearest potassiums are considered, however, a possible explanation for the lack of 180° rotation of octahedral components becomes evident, at least in those parts of the crystals with relatively high potassium contents. In a hypothetical structure where alternate octahedral components were rotated by 180°, *i.e.* alternate use of $\mathbf{V}_1$ and $\mathbf{V}'_1$ vectors, a two-layer hexagonal cell would result, still keeping adjacent potassium ions as far apart as possible, but with a sequence along the *c*-axis of potassium ion/three-membered ring/potassium ion/three-membered ring. . . . . Along the *c*-axis a three-membered ring would therefore be flanked by two octahedral components, both distorted towards it, and second-nearest potassium ions would be closer than in the LZ structure. One might expect this situation to be energetically unfavorable owing to insufficient space between the layers for the three-membered ring in question, and, as with the substitution of manganese

TABLE 3. Observed and calculated $|F|$'s for the two-layer triclinic polytype isolated and in other possible structures

h	k	$\|F\|_{obs}$*	F calc						
			V_1+V_3	V_2+V_9	V_4+V_6	V_5+V_{12}	V_7+V_{10}	V_8+V_8	$V_{11}+V_{13}$
1	0	w	0.48	1.87	1.65	1.33	0.93	0.00	1.99
2	0	s	1.77	1.50	0.71	0.24	1.14	2.00	1.94
$\bar{2}$	1	s	1.77	1.50	0.71	0.24	1.14	2.00	1.94
$\bar{1}$	1	m	1.33	0.93	0.48	1.65	1.99	0.00	1.87
0	1	m	1.14	0.24	1.50	1.94	0.71	2.00	1.77
1	1	s	1.87	0.48	1.99	0.93	1.33	0.00	1.65
2	1	w	0.24	1.14	1.77	0.71	1.94	2.00	1.50
0	2	m	0.71	1.94	0.24	1.77	1.50	2.00	1.14
$\bar{1}$	$\bar{2}$	m-s	1.65	1.99	1.33	0.48	1.87	0.00	0.93
$\bar{1}$	$\bar{1}$	s	1.87	0.48	1.99	0.93	1.33	0.00	1.65
$\bar{1}$	1	m-s	1.33	0.93	0.48	1.65	1.99	0.00	1.37
$\bar{1}$	2	s	1.99	1.65	0.93	1.87	0.48	0.00	1.33

*Observed $|F|$ values: strong (s), medium (m), weak (w)

for iron, any increase in the interlayer spacing to alleviate this would also not be favored. Under such circumstances, therefore, the rhombohedral arrangement would be preferable, but this explanation would clearly not hold for a potassium-deficient structure.

Polytype formation

One of the most significant features in the distribution of polytypes was that they occurred exclusively in at least moderately, or more usually, severely disordered crystals, and although some near-perfect rhombohedral crystals were noted, no near-perfect triclinic polytypes were found. Any mechanism for polytype formation must therefore take into account their apparent connection with the presence of disorder.

Consideration of second-nearest potassium ions, as described above, can be used to explain the formation of the one-layer triclinic structures. If a sequence of consecutive $\mathbf{V}_1$ vectors is broken by a $\mathbf{V}_2$ vector, a region of the crystal around that vector which is very similar to the hypothetical hexagonal structure will be created, although no rotation of octahedral components is involved. This results from the fact that $\mathbf{V}_2$ is very nearly equivalent to $\mathbf{V}'_1$. Considerable strain would result from the interuption of a $\mathbf{V}_1$ sequence in this way, and one might at first expect other, similar mistakes to keep away from the region in question. However, if a second $\mathbf{V}_2$ vector is introduced immediately after the first, and then another *etc.*, a small region of $1Tc(2)$ structure, very similar, regarding the disposition of second-nearest potassium ions, to the alternative rhombohedral $3R(1')$ structure will be set up, and the strain associated with this region will only occur at the boundaries between it and neighboring $3R(1)$ regions. $1Tc(2)$-type regions formed in this manner would therefore always be found with $3R(1)$ regions, as observed, because without the latter there would be no tendency for $\mathbf{V}_2$ vectors to cluster together in the manner found. They would also tend to be associated with a disordered state, owing to the fact that they result from mistakes within a $3R(1)$ region. The comparative scarcity of $1Tc(8)$-type regions then follows from the fact that these vectors lie quite close to the $\mathbf{V}_1$ vector and would therefore create less strain when interspersed in a $\mathbf{V}_1$ sequence. Hence there would be less tendency to build up regular $1Tc(8)$-type regions.

When the crystals become depleted in potassium, the tendency for faults to associate as described above would diminish, producing progressively greater disorder, and an absence of the $3R(1)$ structure, as observed experimentally. Under such conditions, faults could then start to space themselves out evenly throughout the lattice, producing $2Tc(1, 2)$-type structures, if there were sufficient faults to have one at every alternate layer. A possible reason for evenly-spaced faults of this type could arise from the fact that there may be some residual strain in the structure resulting from the presence of three-membered rings. Such strains would be small compared to those created by the presence of potassium ions, and would play no part in determining the stacking sequence when potassium was present, as in the rhombohedral structure successive pairs of three-membered rings superimpose directly. In the absence of

potassium, however, a hexagonal-type structure, with alternate three-membered rings as far apart as possible, could be favored, and if such a structure is, as the experimental evidence appears to indicate, impossible to form, then structures of the $2Tc(1, 2)$-type are a close approximation to it. As the strains involved are much smaller than in the rhombohedral form, there would be more likelihood of these structures being severely disordered, and as such ordering of vectors would occur in potassium-free regions, the formation of $2Tc(1,2)$-type structures in crystals where no rhombohedral form was evident would be favored. Experimental observations tend to confirm this, although the number of crystals displaying this type of structure was relatively small.

Faulting mechanisms

The exact means by which faults are introduced into the structure of zussmanite is open to some speculation, and is almost certainly connected with the means by which the mineral itself forms. If the faults are introduced as zussmanite crystals form in an unoriented fashion from a matrix, it seems improbable that structures involving 180° rotation of octahedral components will not also form, at least in the potassium-deficient regions of the crystals. Another possibility, however, is that zussmanite forms from an existing layer-silicate which already has perfect rhombohedral stacking of layers, and that faults are introduced during a rearrangement of the tetrahedral components. Stilpnomelane occurs associated with zussmanite, and in view of the similar principles upon which the two structures are based, might seem a likely candidate for this role. However, careful examination of several stilpnomelane crystals from the same mineral assemblages revealed no intergrowths with zussmanite, and X-ray studies indicated that rotation of octahedral components in stilpnomelane occurred quite frequently.

An alternative to growth faulting in the manner described above is a true deformation mechanism, occurring after perfect crystals of zussmanite have been formed. Faults could then be introduced by the passage of dislocations with Burgers vectors having components parallel to the octahedra edges through the structure, but in view of the large numbers of faults observed, this might be expected to produce crystals showing the effects of such a shear process. In general, such effects were not visible in the crystals of zussmanite examined in thin section, although in some of the samples there was evidence for a deformation process in some of the coexisting phases. Further investigations on the origin and arrangement of such stacking faults are continuing, especially by lattice resolution techniques, which provide a powerful means of studying the disposition of stacking faults and polytypic modifications. When used in the analytical mode, the electron microscope also provides a means of investigating fine-scale compositional variations, both in zussmanite and in the phases coexisting with it.

Acknowledgments

I should like to thank Dr. M. G. Bown for his constant encouragement and advice throughout the course of this work, and for a critical reading of the final manuscript. Thanks are also due to Dr. S. O. Agrell for providing the specimens used, to Mr. K. O. Rickson and Mr. A. Abrahams for assistance with the X-ray studies, and to Dr. J. V. P. Long and Mr. G. Price for their aid with the electron microprobe analyses. Financial support was received from the Natural Environment Research Council, and this is gratefully acknowledged.

References

AGRELL, S. O., M. G. BOWN AND D. MCKIE (1965) Deerite, howieite and zussmanite, three new minerals from the Franciscan of the Laytonville District, Mendocino County, California, *Am. Mineral.* **50,** 278.

AZAROFF, L. V. (1955) Polarisation correction for crystal-monochromatised X-radiation. *Acta Crystallogr.* **8,** 701–704.

BARBER, D. J. (1970) Thin foils of non-metals made for electron microscopy by sputter-etching. *J. Mater. Sci.* **5,** 1–8.

BRINDLEY, G. W. (1961) X-ray diffraction by layer lattices with random layer displacements. In G. Brown, Ed., *The X-ray Identification and Crystal Structures of Clay Minerals.* Mineralogical Society, London. p. 446–466.

COCHRAN, W. AND E. R. HOWELLS (1954) X-ray diffraction by a layer structure containing random displacements. *Acta Crystallogr.* **7,** 412–415.

EGGLETON, R. A. (1972) The crystal structure of stilpnomelane. Part II. The full cell. *Mineral. Mag.* **38,** 693–711.

GEVERS, R. (1952) Desordre unidimensionnel dans SiC et son influence sur les intensities diffractées des rayons X. *Acta Crystallogr.* **5,** 518–524.

HENDRICKS, S. B. AND E. TELLER (1942) X-ray interference in partially ordered layer lattices. *J. Chem. Phys.,* **10,** 147–167.

HOPE, H. (1971) Polarisation factor for graphite X-ray monochromators. *Acta Crystallogr.* **A27,** 392–393.

JAGODZINSKI, H. (1949) Berechnung des fehlgeordneten dichtesten Kugelpackungen mit Wechselwirkungen der Reichweite 3. *Acta Crystallogr.* **2,** 208–214.

JEFFERSON, D. A. (1973) *A Study of Stacking Disorder in some Silicate Minerals.* Ph.D. Thesis, University of Cambridge.

——— AND M. G. BOWN (1973) Polytypism and stacking disorder in wollastonite. *Nature Phys. Sci.,* **245,** 43–44.

——— AND J. M. THOMAS (1974) High-resolution electron microscopic studies of structural faults in layered silicates. *J. Chem. Soc. Faraday Trans. II,* **70,** 1691–1695.

KAKINOKI, J AND Y. KOMURA (1965) Diffraction by a one-dimensionally disordered crystal. I. The intensity equation. *Acta Crystallogr.* **19,** 137–147.

LOPES-VIEIRA, A. AND J. ZUSSMAN (1969) Further detail on the

crystal structure of zussmanite. *Mineral. Mag.* **37,** 49–59.

MACEWAN, D. M. C., A. RUIZ AMIL AND G. BROWN (1961) Interstratified clay minerals. In G. Brown, Ed. *The X-ray Identification and Crystal Structures of Clay Minerals.* Mineralogical Society, London. p. 393–445.

MEGAW, H. D. (1960) Order and disorder. II. Theory of diffraction effects in the intermediate plagioclase feldspars. *Proc. Roy. Soc. London,* **A259,** 159–183.

MEYER, M. J. (1969) Structur und Fehlordnung des Vaterits. *Z. Kristallogr.* **128,** 183–212.

RADOSLOVICH, E. W. (1963) The cell dimensions and symmetry of layer lattice silicates. IV. Interatomic forces. *Am. Mineral.,* **48,** 76–99.

SHANNON, R. D. AND C. T. PREWITT (1969) Effective ionic radii in oxides and fluorides. *Acta Crystallogr.* **B25,** 925–946.

SHAW, R., R. STEADMAN AND J. D. PUGH (1965) Stacking faults in cronstedtite and other kaolin-type silicates. *Z. Kristallogr.,* **122,** 237–247.

SMITH, J. V. AND H. S. YODER (1956) Studies of mica polymorphs. *Mineral. Mag.* **31,** 209–235.

STOKES, A. R. (1948) A numerical Fourier analysis method for the correction of widths and shapes of lines on X-ray powder photographs. *Proc. Phys. Soc. London,* **61,** 382–391.

SWEATMAN, T. R. AND J. V. P. LONG (1969) Quantitative electron-probe microanalysis of rock-forming minerals. *J. Petrol.* **10,** 332–379.

TAKEDA, H. AND C. W. BURNHAM (1969) Fluor-polylithionite—a lithium mica with nearly hexagonal $Si_2O_5^{2-}$ rings. *Mineral. J. (Japan),* **6,** 102.

WILSON, A. J. C. (1942) Imperfections in the structure of cobalt. II. Mathematical treatment of proposed structure. *Proc. Roy. Soc. London,* **A180,** 277.

WUENSCH, B. J. AND C. T. PREWITT (1965) Corrections for X-ray absorption by a crystal of arbitrary shape. *Z. Kristallogr.* **122,** 24–50.

ZACHARIASEN, W. H. (1947) Direct determination of stacking disorder in layer structures. *Phys. Rev.* **71,** 715–717.

ZHOUKHLISTOV, A. P., B. B. ZVYAGIN, S. V. SOBOLEVA AND A. F. FEDOTOV (1973) The crystal structure of the dioctahedral mica $2M_2$ determined by high voltage electron diffraction. *Clays Clay Miner.* **21,** 465–470.

Manuscript received, December 23, 1974; accepted for publication, December 12, 1975.